Improving Grid-Connected Tidal Power Systems Through PWM Inverters Based on Voltage-Oriented Control

L. M. Kangaji[1*], E. Orumwense[2], A. Raji[1]
[1]Electrical Engineering, Peninsula University of Technology, Cape Town, 7535 2, South Africa
[2]Mechanical Engineering Department, Peninsula University of Technology, Cape Town, 7535 2, South Africa
[*]Corresponding author's email: laskangaji@gmail.com

Abstract – *Pulse width modulation (PWM) rectifiers play a critical role in AC to DC power conversion for renewable energy applications. Existing systems predominantly employ basic voltage-oriented control (VOC) strategies and conventional 2-level converters, which often face challenges such as suboptimal steady-state performance, slower transient response, and elevated harmonic distortions. Moreover, these systems typically lack sophisticated control mechanisms for managing active and reactive power, thereby potentially compromising overall efficiency and stability. This proposed voltage-oriented control strategy aims to overcome these limitations by enhancing both steady-state performance and transient response through an inherent current control loop. Specifically, in the context of grid-connected tidal energy systems, the generator side utilizes field-oriented control (FOC), while the grid side employs a 3-level H-bridge voltage source converter integrated with VOC and a phase-locked loop (PLL). These advanced control strategies are designed to optimize power extraction and more effectively manage active and reactive powers. MATLAB/Simulink simulations have been conducted to validate the efficacy of the proposed controller, demonstrating its ability to ensure system stability, reduce harmonic distortions, and manage reactive power effectively. The system, featuring a 1.5 MW/C, 1.2 MW three-level inverter, and LCL filter, achieves harmonic distortion below 5%, showcasing the filter's efficiency. The comprehensive simulation results support the feasibility and effectiveness of the proposed voltage-oriented control strategy, addressing total harmonic distortion (THD), dynamic performance, and parameter sensitivity.*

Keywords: *Harmonic reduction, power quality, PWM rectifier, Tidal energy, Voltage control*

Article History
Received 12 July 2024
Received in revised form 8 September 2024
Accepted 7 October 2024

I. Introduction

Integrating renewable energy sources, such as wind and tidal power, into the utility grid introduces a range of technical and economic challenges [1]. These challenges encompass power quality issues, including reliability, harmonics, voltage stability, control, protection, frequency regulation, and reserve allocation [2] – [3]. Additionally, the grid's inherent voltage harmonics can distort the current supplied [4]. Tidal energy systems, in particular, face significant hurdles due to the unpredictability of tidal speeds and difficulties in directly connecting to the traditional grid, which requires a meticulous integration process [4] – [5]. Effective control of power converters and conditioning processes is essential to address these issues [6].

Tidal energy systems, while sharing similarities with offshore wind turbines, have distinct characteristics that necessitate specialized solutions [7] – [8]. These include the predictable nature of tidal currents, reduced swept areas due to higher water density, and shorter distances to shore [9]. Vienna converters, known for their low harmonic distortion, high efficiency, and impressive power density, have emerged as a noteworthy solution in renewable energy applications, particularly in wind power systems [10]. Various control strategies, such as proportional-integral (PI) control, proportional resonant control, and sliding mode control, are utilized to enhance the performance of Vienna rectifiers [11]. However, the unidirectional operation of Vienna rectifiers limits their capability to generate reactive power [12], which is crucial for effective grid integration of wind and tidal energy [13].

In contrast, Pulse Width Modulation (PWM) rectifiers offer several advantages, including effective power quality management, high power factor, and bi-directional flow capability [14]. The traditional control strategy for

PWM rectifiers employs a synchronous rotating reference frame with decoupled PI controllers, but it faces challenges related to slow dynamic response [15]. Voltage-Oriented Control (VOC) is a prominent technique in PWM rectifiers, optimizing performance by managing direct and quadrature axis currents to regulate active and reactive power[16]. Direct Power Control (DPC) approaches have also gained attention for their ability to directly control active and reactive power [17].

Integrating PWM rectifiers with VOC in tidal generation systems provides significant benefits [18], including improved power quality, reduced harmonic distortions, and enhanced power factor [19]-[20]. This integration addresses the variable nature of tidal energy, ensuring efficient energy transfer and stability within the grid [21].

Aims:

- Enhance Power Extraction Efficiency: Optimize the extraction of power from tidal energy systems by applying vector-oriented decoupling control on the generator side.
- Implement Voltage-Oriented Control: Develop and apply voltage-oriented control techniques to effectively manage active and reactive power in grid-connected tidal power systems using PWM inverters.
- Analyze Simulation Outcomes: Perform a detailed analysis of simulation results to evaluate the performance of PWM inverters with voltage-oriented control, focusing on their impact on grid stability, power quality, and overall system efficiency.

TABLE I
PARAMETERS OF THE 300 KW HORIZONTAL AXIS TIDAL STREAM TURBINE (HATST) PROTOTYPE.

Parameter	Value
Radius	8.5 m
Maximum pitch angle	8°
Rated power	300 kW
Rated flow velocity	2 m/s
Rated rotational speed	12 rpm
Optimal TSR	5
Starting flow velocity	0.7 m/s
Total maximum efficiency	≥30%

The equation for estimating the power capacity of tidal currents can be derived by utilizing the identical formula applied in wind energy systems. In this equation, P denotes power measured in Watts (W); represents the device efficiency or power coefficient; **ρ** represents the water density, typically estimated at approximately 1025 Kg/m^3; A stands for the swept area in square meters (m^2), and U signifies the current velocity measured in meters per second (m/s), as depicted in Equation (1).

$$P = \frac{1}{2}\rho C_p A V_{tides}{}^3 \quad (1)$$

The modelling of the generator side includes an explanation of the rotor model. In this context, the rotor design assumes a crucial role in determining the amount of mechanical power (P_m) generated from the energy of the tidal stream. It's important to note that the power coefficient C_p is intricately linked to this rotor design. The rotor model is described as part of the modelling of the generator side.

$$P_m = C_p P_{tide} \quad (2)$$

$$P_m = \frac{1}{2} C_p \rho A V^3 \quad (3)$$

The power of the tidal stream is therefore divided by the power coefficient to determine the mechanical power output:

In this instance, the C_p maximum value of 0.44 is approximated indicates in Fig. 1. The power coefficient's value is contingent upon both the tip speed ratio and the pitch angle. However, in the case of fixed-pitch systems, the power coefficient C_p is solely determined by the tip speed ratio. This ratio elucidates the connection between the rotational speed of blades with radius 'r' and the velocity of the water v:

$$\lambda = \frac{\omega_m r}{v} \quad (4)$$

The $C_P(\lambda)$-curve has undergone experimental validation across TSR values ranging from 2.9 to 4.5, with flow velocities falling within the 1.2 to 1.4 m/s range, as detailed in [10]. The curve derived from the experimental data is depicted in Fig. 1 and is mathematically represented by the equation = $C_P(\lambda)$-$0.0836\lambda^2 - 0.0183\lambda^3$ (5). The calculated optimal tip speed ratio from this power coefficient curve is approximately λopt ≈ 3.05, corresponding to an optimal power coefficient of $C_p(\lambda_{opt}) \approx 0.26$.

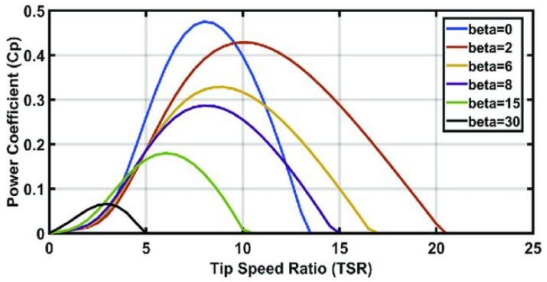

Fig. 1: Power Coefficient with Tip Speed Ratio (TSR) and Blade Pitch Angle.

II. Rectifier and Control systems

Rectifiers are crucial in converting alternating current (AC) to direct current (DC) within hybrid energy systems. This section provides a detailed exploration of rectifiers, focusing on their essential parameters and control techniques to ensure efficient operation and integration.

A. PWM Non-Regenerative Rectifiers

PWM non-regenerative rectifiers are electronic devices that convert AC power to DC power with high efficiency and controlled output. "PWM" stands for Pulse Width Modulation, a technique used to regulate the output voltage and current by adjusting the width of the voltage pulses.

"Non-regenerative" refers to the inability of these rectifiers to feed energy back into the power source; they can only convert power in one direction, from AC to DC. This is contrasted with regenerative rectifiers, which can also return power to the grid or source when needed.

PWM non-regenerative rectifiers are commonly used in applications requiring controlled DC power, such as in DC motor drives, battery charging systems, and various industrial processes. They offer advantages such as improved power quality, reduced harmonic distortion, and high power factor compared to traditional rectifiers. However, they are limited by their inability to handle energy regeneration or power reversal [11].

B. PWM Three-phase Boost Rectifier

Due to its asymmetric current-drawing characteristics, the three-phase boost rectifier is frequently recommended for high-power applications. This topology is widely adopted because boost converters can achieve near-unity power factors and exhibit low distortion in line currents under diverse load conditions [18]. Despite these advantages, a notable drawback extensively reported in the literature is the potential for output voltage instability. Such instability can detrimentally impact the system's overall reliability and efficiency, especially under varying operating conditions. Therefore, it is imperative to incorporate meticulous design considerations and implement robust control strategies to mitigate voltage fluctuations and ensure consistent system performance [22].

C. PWM Three-phase Vienna

The Vienna rectifier architecture, illustrated in Fig. 2, comprises six active semiconductor switches, which can be either Insulated Gate Bipolar Transistors (IGBTs) or Metal-Oxide-Semiconductor Field-Effect Transistors (MOSFETs), and six diodes. Each diode and switch are subjected to a voltage stress of Vdc/2. The architecture employs three inductors on the AC input side and two parallel capacitors on the DC side. The neutral point of the DC link is connected to the grid's neutral point. Despite the advantages offered by this architecture, its practical implementation necessitates sophisticated control schemes and may require the fabrication of specialized semiconductor modules [13].

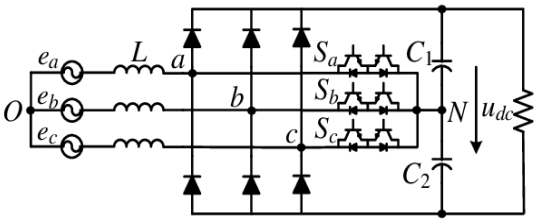

Fig. 2: A three-phase Vienna rectifier.

Regenerative rectifiers are advanced power conversion devices capable of bidirectional power flow. In rectifier mode, they convert AC power to DC, while in reverse operation, they act as inverters, converting DC back to AC. This dual functionality is crucial for applications requiring bidirectional energy transfer, such as motor drives, high-voltage direct current (HVDC) transmission systems, and tidal turbine grid integration.

In these contexts, regenerative rectifiers enable efficient energy recovery and reintegration into the power grid, thereby enhancing system efficiency and stability. Their ability to return excess energy to the source helps in managing power flow, improving power quality, and ensuring seamless operation across varying load and generation conditions. This capability is particularly important in modern electrical systems that prioritize energy conservation and efficient resource utilization [23].

D. Carrier-based sinusoidal pulse-width modulation (SPWM)

Sinusoidal pulse-width modulation (SPWM) is widely employed by power electronics professionals to control the output of inverters, particularly in renewable energy applications like offshore tidal power systems. SPWM utilizes a triangular carrier wave to generate the PWM signals. Originally developed for three-phase voltage source inverters (VSIs), this technique has been adapted for three-phase current source rectifiers and, in some instances, for voltage source rectifiers [24]. For efficient operation, the PWM pattern must generate a sinusoidal waveform that matches the frequency of the input voltage. By adjusting the amplitude and phase of the PWM sinusoid, the system can accommodate both leading and lagging power factors in rectifier and inverter operations, enhancing the versatility and performance of the system.

Refer to Fig. 3 for an illustration of this modulation technique [25].

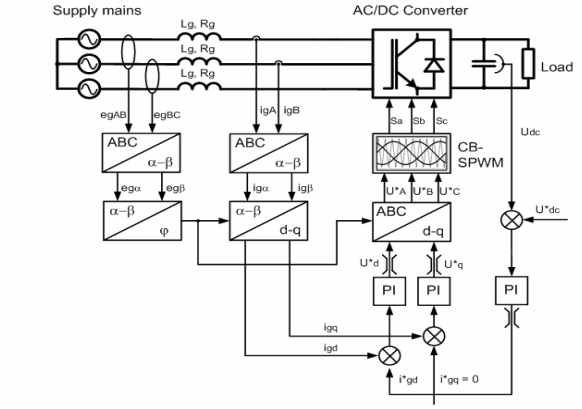

Fig. 3: Voltage-Oriented Control with CB-SPWM

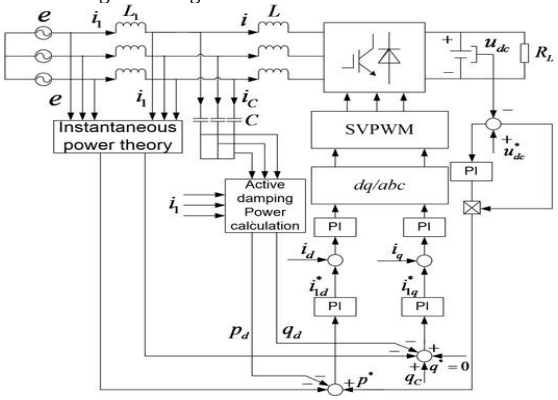

Fig. 4: Direct Power Control of PWM Rectifier with LCL Filter Using Power Damping Feedback.

The equations for stator voltage in a fixed reference frame are provided as follows [26]:

E. Voltage-Oriented Control (VOC) Framework

Voltage-Oriented Control Approach:

The Voltage-Oriented Control (VOC) strategy is employed to precisely regulate the output DC voltage of the inverter by controlling the current within the system [27]. VOC operates by projecting the three-phase voltage and current variables of the Voltage Source Inverter (VSI) onto a synchronously rotating dq-frame, which facilitates effective control of both active and reactive power. The key components of VOC are [22],[28]:

- Inner Current Control Loop:

This loop regulates the DC-link voltage by setting the reference currents for the inner loop [29].

- Outer Voltage Control Loop:

This loop ensures the DC-link voltage maintains a value close to the reference, adapting dynamically to variations [29].

F. Mathematical Equations:

- Voltage Equations in dq-frame:

$$[V_{abc}] = [R][i_{abc}] + [L]\frac{d(i_{abc})}{dt} + \frac{\lambda abc}{dt} \quad (5)$$

$$\begin{cases} \mathrm{V_d} = \mathrm{R_{id}} + \mathrm{L_d}\dfrac{\mathrm{di_d}}{\mathrm{dt}} - \mathrm{L_q i_q \omega_s} \\ \mathrm{V_q} = \mathrm{Ri_q} + \mathrm{L_q}\dfrac{\mathrm{di_d}}{\mathrm{dt}} + (\mathrm{L_d i_d} + \phi_\mathrm{m})\omega_\mathrm{s} \end{cases} \quad (6)$$

Where $\mathrm{V_d}$and $\mathrm{V_q}$ are the direct and quadrature axis voltages, I_d and I_q the direct and quadrature axis currents, R is the resistance, and L is the inductance [23], [30].

- Power Equations:

$$P = V_d I_d + V_q I_q \quad (7)$$

$$Q = V_d I_d - V_q I_q \quad (8)$$

where P is the active power and Q is the reactive power.

G. Direct Power Control (DPC) of PWM Rectifier

Characteristics of DPC:

- Instantaneous Power Regulation:

Directly regulates both active and reactive power, enhancing power conversion efficiency.

- Power Damping Feedback:

Utilizes feedback to stabilize power and mitigate oscillations and disturbances.

- Harmonic Mitigation:

Incorporates an LCL filter to minimize PWM-induced harmonics, improving power quality.

- Enhanced Dynamic Performance:

Adapts quickly to changes in load and grid conditions.

- Simplified Control Structure:

Reduces control complexity while enhancing system reliability.

- *Permanent Magnet Synchronous Generator (PMSG) Model*

Electromagnetic Torque:

$$T_{em} = \frac{3}{2}\frac{P}{2}(\psi_f I_q - L_d I_d) \quad (9)$$

where T_{em} is the electromagnetic torque, P is the number of pole pairs, ψ_f is the flux linkage, and L_d is the direct-axis inductance.

- Mechanical Dynamics:

$$\frac{d\omega_m}{dt} = T_{em} - T_{load} \quad (10)$$

where J is the moment of inertia, $d\omega_m$ is the mechanical speed, and T_{load} is the load torque.

- *Simplified Torque Equation:*

Electromagnetic Torque:

$$T_{em} = \frac{3}{2}\frac{P}{2}(\psi_f I_q - L_d I_d) \quad (11)$$

- *LCL Filter Modelling*

LCL Filter Parameters:

- Impedance and Capacitance:

$$Z_{LCL} = \frac{V_g}{I_{LCL}} \quad (12)$$

$$C_{filter} = 0.05.C_{base} \quad (13)$$

where V_g is the grid voltage, I_{LCL} is the current through the LCL filter, and C_{base} is the base capacitance.

- *Active Filter Function (AFF) for Harmonic Compensation:*

Harmonic Compensation:

$$i_{comp} = i_{measured} - i_{reference} \quad (14)$$

- *Current Ripple Estimation*

Current ripple estimation involves determining fluctuations in electrical current caused by switching in power converters, crucial for minimizing harmonic distortion, improving efficiency, and ensuring power quality and system stability [8].

- *Current Ripple Formula:*

The maximum current ripple at the inverter output can be estimated using:

$$\Delta I_{ripple} = \frac{V_{DC}(1-m)}{L.f_s} \quad (15)$$

where ΔI_{ripple} is the DC bus voltage, mmm is the modulation index, L is the inductance, and f_s is the switching frequency.

- *Voltage-Oriented Control Implementation*

Control Strategy:

- Outer Voltage Control Loop:

$$V_{DC,ref} = V_{DC} + K_p\left(V_{DC,ref} - V_{DC}\right) \quad (16)$$

where K_p is the proportional gain.

- Inner Current Control Loop:

$$I_{d,ref} = \frac{V_{DC} - V_{DC,ref}}{R} \quad (17)$$

$$I_{d,ref} = \frac{V_{q,ref}}{L} \quad (18)$$

- *Minimum DC-Link Voltage:*

To ensure proper operation, the minimum DC-link voltage must be calculated as [27]:

$$V_{DC,min} = \sqrt{3}.V_{line-to-ground} \quad (19)$$

- DC-Link Capacitor Calculation:

The DC-link capacitor C_{DC} is determined by:

$$C_{DC} = \frac{P}{V_{DC}.f\Delta V_{DC}} \quad (20)$$

ΔV_{DC} is the maximum ripple in DC voltage, P is the active power, and f is the generator frequency [22],[28].The specific parameters for the LCL filter and the PWM regenerative rectifier modelling parameters are outlined in Table 2 and Table 3:

TABLE II
THE LCL FILTER PARAMETERS

Parameters	Values
Inverter side inductor	*0.9mH*
Grid side inductor	*0.072mH*
Capacitor filter	*531μF*
Damping Resistor	*0.118*Ω
Resonant frequency	*845Hz*
Inductor resistances	*0.00761*Ω
Sampling frequency	*10,000Hz*
Crossover Frequency	*254 Hz*

TABLE III
THE PWM REGENERATIVE RECTIFIER MODELLING PARAMETERS.

Parameters	Values
V_{dc}	1500 V
V_{ll}	600 V
C_{DC}	150 V0.04 Farad

H. Generic Three-Phase VSC Electrical Topology

The configuration of a generic three-phase Voltage Source Converter (VSC) electrical topology is illustrated in Fig. 5. The system setup includes a voltage source rectifier with line inductance on the AC side (*L*s, *R*s), six individual IGBT switches, and a DC-link capacitor C on the DC side [31].

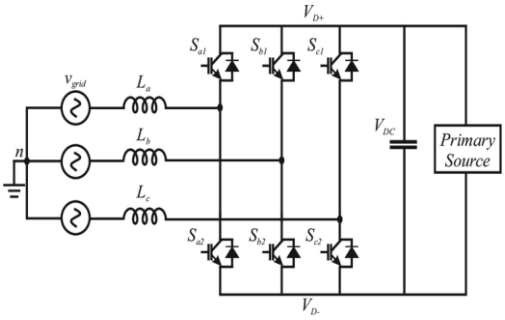

Fig. 5: Generic Three-phase VSC electrical topology [32].

$$V_{(DC-min)} > \sqrt{2}\sqrt{3}V_{LN(rms)} = \sqrt{3}E_m \quad (21)$$

The $V_{(DC-min)}$ represents the minimum DC-Link voltage, and$V_{(rms)}$ is defined as the line-to-ground voltage. This analysis determines the minimum DC-link voltage through equation (21), presented as follows. Taking the maximum reference voltage as $\frac{V_{DC}}{2}$, Equation (22) can be expressed as shown:

$$V_{(LNpeak)} = \frac{V_{DC}}{2} \quad (22)$$

$$V_{(DC-min)} > 2V_{LN(peak)} = \frac{2\sqrt{2}}{\sqrt{3}}V_{LN(rms)} = 1.663VLL(rms) \quad (23)$$

The DC link voltage is considered inconsistent with Equation (21). The calculation of the DC-link capacitor can be determined using the following equation:

$$C_{DC} = \frac{P}{2\pi f V_{DC}\Delta V_{DC}} \quad (24)$$

Here, ΔV_{DC} denotes the maximum ripple in DC voltage, typically approximately 5% of the supply voltage, where V_{DC} is the DC bus voltage. Additionally, P represents the active power, and f corresponds to the generator frequency.

III. Methodology

This study leverages MATLAB/Simulink for modeling and optimizing grid-connected tidal power systems using voltage-oriented control (VOC). The methodology includes transforming the power coefficient curve into a mathematical representation and implementing discretely tuned PI controllers with anti-windup features. Designed specifically for tidal Stream Energy applications, the system comprises a PWM rectifier and a 2-level voltage source converter (2L-VSC) to convert AC to DC, enhanced by a harmonic LC filter for superior output quality. Grid integration is facilitated through a 3-level cascaded H-bridge VSC, controlled by VOC coupled with a phase-locked loop (PLL). The VOC algorithm utilizes a decoupler and three PI controllers to manage current components and DC-link voltage. Key system components—tidal generator, filter, converter, rectifier, and grid—are illustrated in Fig. 6

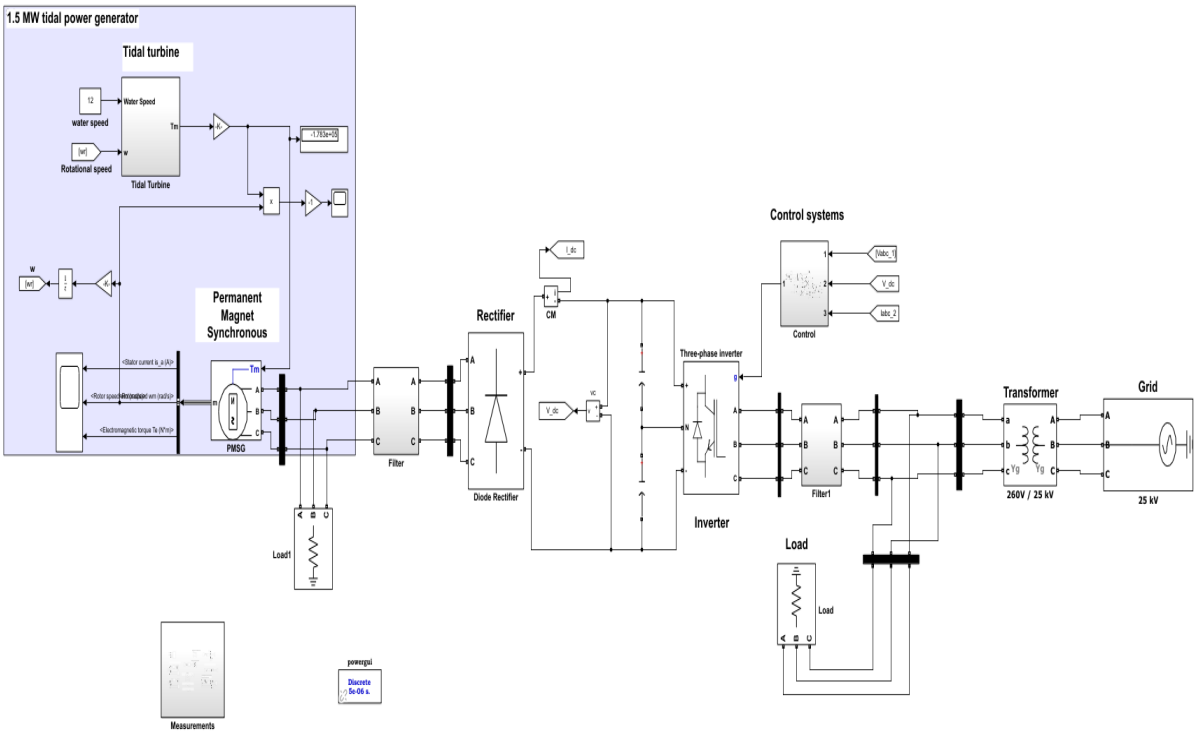

Fig. 6: Grid-connected PMSG-based tidal generation system

IV. Results and discussion

This study proposes using the simplified network depicted in Figs. 3 and 4 to evaluate the improved power quality achieved by connecting a voltage-oriented PWM rectifier to a grid-connected tidal turbine. The system integrates a tidal turbine shaft with a Permanent Magnet Generator (PMG) rotor and a full-scale power converter connected to the grid via a Permanent Magnet Synchronous Generator (PMSG). Three-phase undersea cables transmit the 6.6 kV output from the Medium Voltage (MV) generator to shore, where an onshore transformer typically steps down the voltage to a Low Voltage (LV) transmission level (690 V).

TABLE V
TIDAL GENERATOR MODELLING PARAMETERS

Parameters	Value
P_{nom}	1.5 MW
V_{nom}	600 V
R_s	0.006
L_{dq}	0.3e-3
ϕ	1.48
J	35000
Viscous Damping	0.01
Friction	0
N_p	48

The tidal generator's reactive power generation and active power output, estimated at 1.324 MW, are depicted in Figs: 7a and 7b. The simulation shows a significant negative undershoot of approximately 69.62%, a minor positive undershoot of around 1.055%, and a substantial overshoot of 233% during the initial phase.

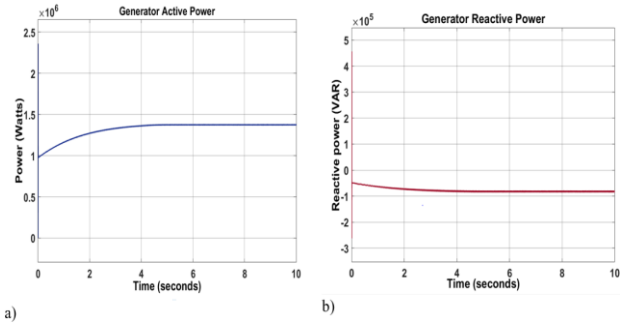

a) b)

Fig. 7: (a) Active power output from the tidal generator and (b) the reactive power generated by the tide generator.

The active and reactive power curves at the load output terminals are illustrated in Fig. 8. The active power is recorded at 2.5 MW, while the reactive power remains near zero (1.865 × VAR). After this period, the response stabilizes, maintaining a consistent output of 917 kW. Fig. 8 displays the active and reactive power exported to the grid. The grid-connected inverter is required to supply 508.4 KVAR of reactive power and approximately 573.9 kW of active power to the tidal energy system.

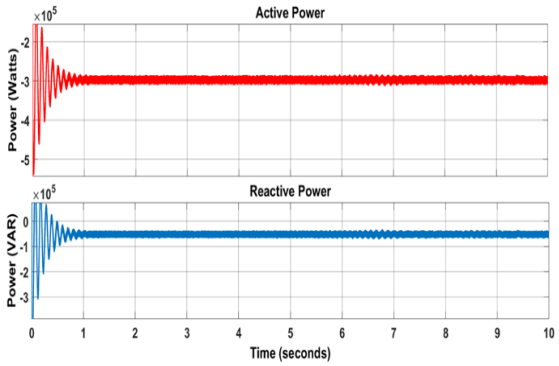

Fig. 8. Active and Reactive Power

A. Inverter Characteristics

Multilevel voltage-source inverter (VSI) technology is commonly utilized in grid-connected tidal energy conversion systems (TCS), as illustrated in Fig. 5. Due to the inherent buck characteristics of Voltage Source Inverters (VSIs), a boost converter is required to elevate the DC-link voltage when the VSI is utilized as the power conversion circuit in a TCS.

Fig. 9 illustrates the phase-to-phase voltage of a three-level inverter, revealing the harmonics introduced by inverter switching. These harmonics can substantially degrade system efficiency, resulting in transient effects and a diminished power factor. To maintain acceptable system performance, the total harmonic distortion (THD) must be kept below 5% for voltages ranging from 1 to 68 kV. The current harmonic distortion threshold is set at a higher value, with a minimum of 1000 A.

To reduce the harmonics, an LCL filter is installed between the grid and the inverter. Voltage and current signals have harmonics that exceed the usual system frequency of 50 Hz.

The output of the LCL filter, illustrating the phase-to-phase voltages and currents, is also shown in Fig. 9 and Fig. 10.

Phase currents are approximately 1213 A, while voltage magnitudes are around 600 V. The phase-to-phase voltage has an undershoot of 1.985% and an overshoot of 0.324%, with a rising time of approximately 5.853 milliseconds and a fall time of 5.837 milliseconds. Similarly, the phase current exhibits rise and fall periods of 5.819 and 5.823 milliseconds, with overshoot and undershoot values of 1.99%. These metrics indicate that harmonic distortion is effectively reduced by the implemented LCL filter, ensuring that performance standards are met.

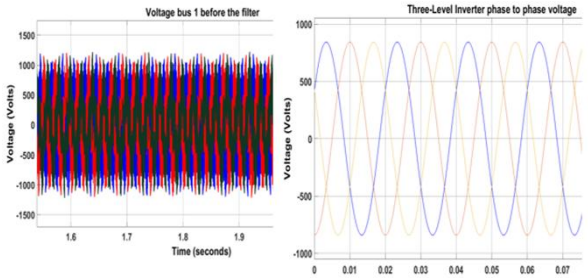

Fig. 9.The three-phase voltage before the filter

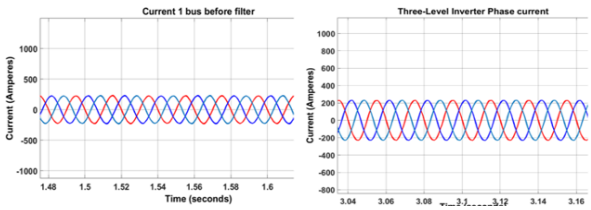

Fig. 10: The three-phase voltage before the filter, Current before the filter

The voltage control method utilized in this study compares the DC link voltage to a reference voltage set at 1500 V. The currents $I_q$and $I_{qreference}$ (I_{dref}) are evaluated through the current PI controller on the q-axis, generating the voltage V_q based on the error between the two currents.

The $V_{qreference}$ is maintained at zero,$I_{dreference}$ (I_{dref}) in Fig. 13e, representing the DC link. Fig. 11d illustrates the actual and reference voltages of the DC link. The model controls outperform expectations, with little difference between the actual and reference signals. However, overshoots occur at simulation states 14, 688, and 15, after which both voltages normalize. Fig. 12e compares the current. The current (I_d) and the current reference (I_{dref}) are compared in Fig. 13e.

The current PI controller generates the voltage (V_q) on the q-axis by comparing the actual and reference currents. The I_q reference value is kept close to zero. The grid voltage in the dq0 frame is crucial for generating the voltage required to detect the modulation signal. The grid regulates its reactive power by setting the d-axis voltage to 500 V while keeping the q-axis value at zero. Figs. 13a and 13b show the voltages in the dq0 frame (I_d and V_q), which help to examine the modulation signal, as well as the estimated values for the d and q axes. The modulation signal's findings on both axes are calculated with a modulation index of 0.7. The modulation signals are then transformed from the dq0 frame to the ABC frame and delivered to the pulse width modulation (PWM) generator, producing the twelve pulses required for operating the three-level system.

The phase-locked loop (PLL) indicates in Fig. 14 plays a crucial role in this process by generating an output signal that is synchronized with the phase of the input. The PLL employs an internal frequency oscillator to continuously

track the frequency and phase of a sinusoidal three-phase signal, thereby minimizing phase differences and ensuring synchronization. As depicted in Fig. 13, the PLL frequency (f) is set to 50 Hz, aligning closely with the grid frequency with only minor deviations. The PLL accurately detects the grid voltage and phase angle through dq0 frame current control synchronization, ensuring optimal alignment between the inverter and the grid.

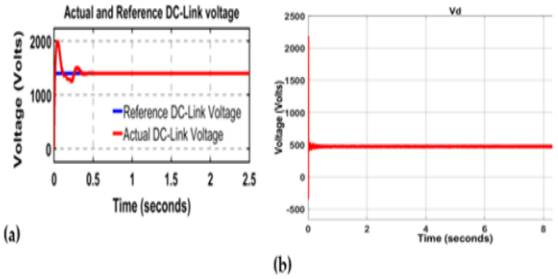

Fig. 11: (a) Actual and Reference DC-link voltage, and (b) V_d

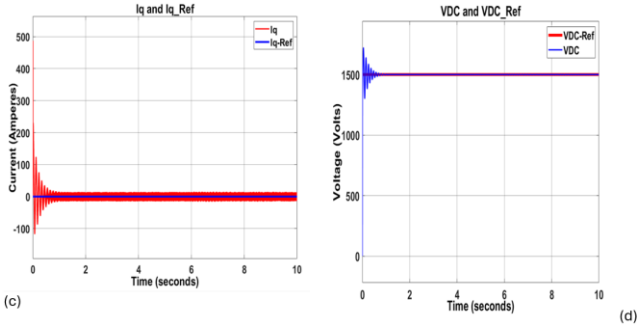

Fig. 12: (c) I_q and I_q-ref, and (d) V_{DC}, $V_{DC\ ref}$

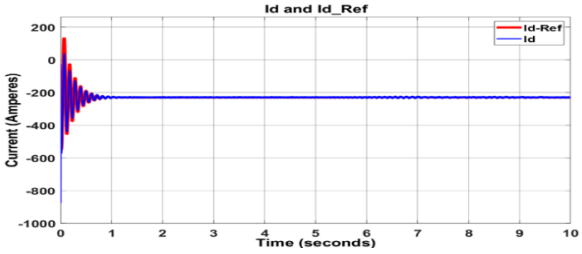

Fig 13. I_d and I_{dRef}

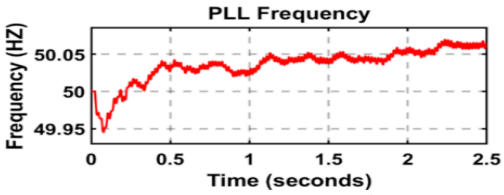

Fig. 14:Phase-locked loop (PLL) frequency

The inverter has been precisely constructed to generate a grid-compatible voltage. This three-level inverter maintains a constant voltage level regardless of the control and load factors. It efficiently converts the DC-link voltage into a three-level AC voltage that oscillates between -VDC and +VDC, as shown in Fig. 11 (a) and (b). This AC voltage is used as the inverter's output, avoiding the requirement for a filtering mechanism. The peak-to-peak voltage and root mean square (RMS) value are 938 volts. The waveform reaches approximately 2800 V, with maximum and minimum values of +1400 V and -1400 V, and it shows pulses of varying widths depending on signal amplitude. The fundamental frequency of the waveform is exactly 50 Hz, which corresponds to the grid frequency. The phase-to-phase voltage has a rising period of 3.841 milliseconds and a fall time of 3.971. The overshoot and undershoot rates are 0.49% and 25.347%, respectively.

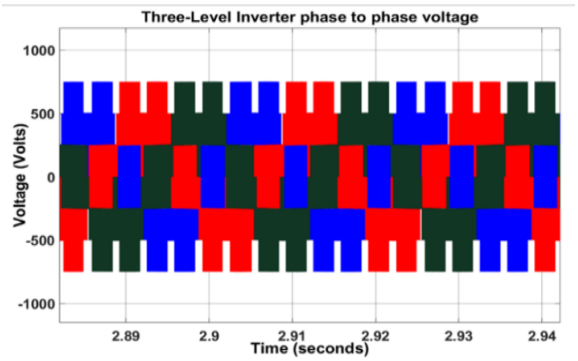

Fig. 15: Inverter phase-to-phase voltage.

The phase-to-phase voltage generated by the three-level inverter, as shown in Fig. 15, exhibits harmonic distortions caused by the switching operations of power electronic devices within the inverter. Harmonics in offshore tidal systems can degrade power quality, causing voltage and current distortion. This leads to increased losses, equipment stress, and reduced lifespan. Harmonics can also interfere with communication systems, contribute to grid instability, and cause regulatory compliance issues. Ensuring harmonic mitigation is essential to maintain system efficiency and reliability. Specifically, IEEE 519-2014 demonstrates that the total harmonic distortion (THD) for voltages ranging from 1 to 68 kV should not exceed 5%, while the allowed THD limit for currents greater than 1000 A is 20%.

Fig. 16 (a) and (b) present the THD analysis before filtering, revealing a significant THD of 42.35.38% in the phase-to-ground voltage waveform and 11.54% in the phase current signal. As indicated in Figs. 15, effective filtering procedures significantly reduce THD values to 0.07% for current and 0.12% for voltage. This reduction demonstrates the effectiveness of the filtering approaches in lowering harmonic distortions to levels well within the IEEE-specified limits. Such measures are critical for maintaining compliance with grid connection standards, optimizing system performance, and mitigating potential negative effects on grid stability and reliability. Future developments in inverter design and control strategies will continue to prioritize minimizing harmonic content to

enhance overall power quality in grid-integrated renewable energy systems.

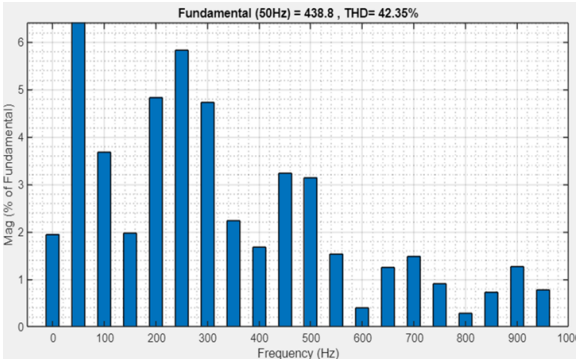

Fig. 16. (a) Voltage, (b) Current Total Harmonics Distortion.

Two case studies were conducted to evaluate the performance of a tidal generation system under different load conditions. These studies examined scenarios where the load was below or above the system's tidal energy output capability. Key parameters such as active and reactive power, grid voltage, and current were analyzed across various operational modes (see Figs. 18–19).

In the scenario where the load demand was smaller than the tidal energy system's output capacity (Fig. 18), despite the system's maximum output of 1.54 MW, a 2.5 MW load was connected to the grid-connected tidal power system. To meet this demand, an additional 1.23 MW of power was imported from the grid using an inverter with 88% efficiency.

Fig. 20 depicts the patterns of active and reactive power at the load terminals. The reactive power fluctuated around zero (1.865 × VAR), and the active power steadied around 2.5 MW. The active power signal showed a 14.557% overshoot between t = 0 and t = 0.3 s, followed by a 1.998% undershoot between t = 0.3 and t = 0.4 s, before stabilizing at around 917 kW. In terms of electricity exported to the grid (Fig. 18), the tidal energy system exported approximately 573.9 kW of active power and was expected to create approximately 508.4 KVAR of reactive power from the grid-connected inverter. The active power signal had a delay of 61.950 milliseconds, with 10.92% overshoot and 8.35% undershoot. Reactive power showed a delay of about 29.842.

Fig. 19 displays the phase currents and phase-to-phase voltages at the load terminals as pure sinusoidal waves. The RMS voltage was set at approximately 600 V, with currents expected to be around 874.4 A. The voltage rise and fall times were about 5.854 and 5.858 milliseconds, respectively, with a 1.983% overshoot and undershoot. Current rise and fall times were approximately 5.858 and 5.855 milliseconds, respectively, with a 0.312% overshoot and a 1.984% undershoot.

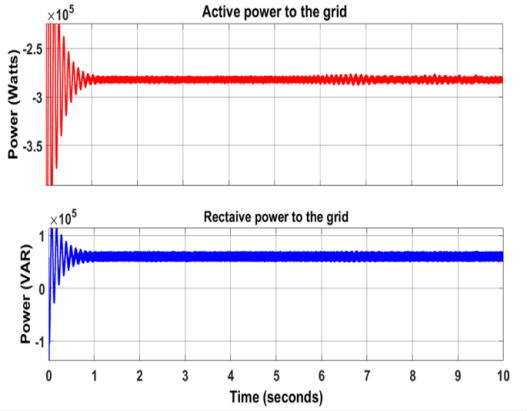

Fig. 16: Grid active power and reactive power

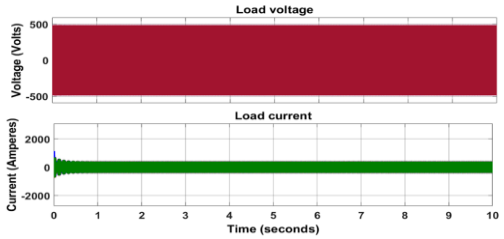

Fig. 17: Indicates Load voltage and load current.

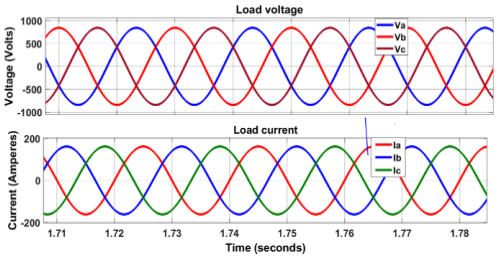

Fig. 18: Indicates load voltage and load current.

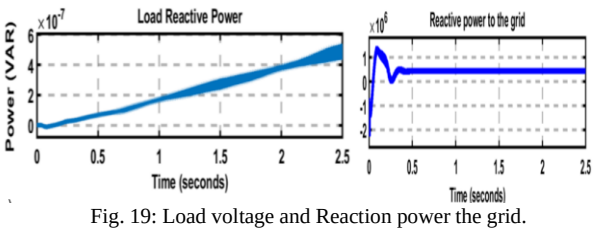

Fig. 19: Load voltage and Reaction power the grid.

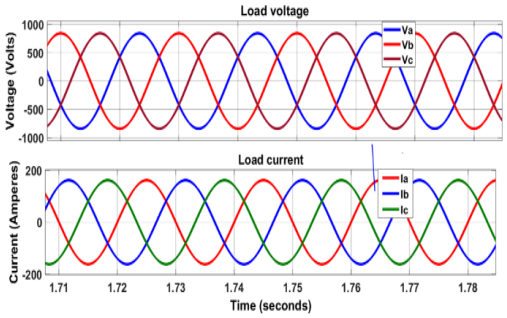

Fig. 20: Indicates load voltage and load current.

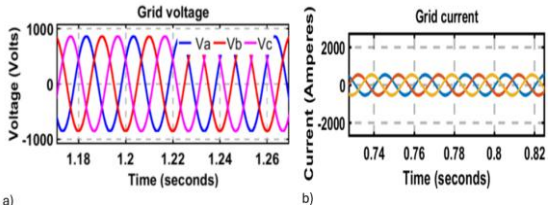

Fig. 21: (a) Grid voltage, and (b) Grid current.

V. Conclusion

This research paper has presented a thoroughly designed and validated three-level Pulse Width Modulation (PWM) rectifier, integrated with an advanced voltage-oriented controller (VOC). Through rigorous simulations using MATLAB Simulink software, the study has focused on high-power applications within the realm of grid-connected tidal generation systems.

The implementation of voltage-oriented control in conjunction with Carrier-Based Sinusoidal PWM has significantly advanced grid-connected tidal power systems. This approach, specifically tailored for high-power scenarios, proves highly effective for tidal energy systems in coastal cities.

The integration of the proposed system with Carrier-Based Sinusoidal PWM, along with meticulously designed input and output filters, has addressed key challenges related to reactive power and unstable active currents. The combined operation of the voltage-oriented controller (VOC) and the PWM rectifier ensures that sinusoidal currents with minimal ripples and distortions are maintained at the input side. Additionally, the system achieves a unity power factor, with the total harmonic distortion of the input current consistently below 5%, meeting the stringent IEEE-519 standard requirements.

Acknowledgements

The authors would like to express their gratitude to the Cape Peninsula University of Technology (CPUT) for providing comprehensive support and resources for this research.

Conflict of Interest

The authors declare that they have no known competing financial interests or personal relationships that could have appeared to influence the work reported in this paper.

Author Contributions

Author 1 designed and simulated the three-level PWM rectifier, developed the VOC model in MATLAB Simulink and wrote the methodology and results sections. Author 2 optimized the Carrier-Based Sinusoidal PWM, designed input and output filters, and contributed to control strategies and the discussion and conclusion sections. Author 3 oversaw the project, ensured IEEE-519 compliance, and reviewed the manuscript, providing feedback and final approval for submission.

References

[1] S. P. Neill *et al.*, "Tidal range energy resource and optimization – Past perspectives and future challenges," *Renew. Energy*, vol. 127, pp. 763–778, 2018, doi: 10.1016/j.renene.2018.05.007.

[2] N. K. Roy and H. R. Pota, "Current Status and Issues of Concern for the Integration of Distributed Generation into Electricity Networks," *IEEE Syst. J.*, vol. 9, no. 3, pp. 933–944, 2015, doi: 10.1109/JSYST.2014.2305282.

[3] F. R. Islam, A. Lallu, K. A. Mamun, K. Prakash, and N. K. Roy, "Power Quality Improvement of Distribution Network Using BESS and Capacitor Bank," *J. Mod. Power Syst. Clean Energy*, vol. 9, no. 3, pp. 625–632, 2021, doi: 10.35833/MPCE.2019.000304.

[4] A. Angeloudis, S. C. Kramer, and A. Avdis, "Optimising tidal range power plant operation," pp. 1–24, 2017.

[5] Z. Lin, X. Ruan, L. Wu, H. Zhang, and W. Li, "Multi resonant Component-Based Grid-Voltage-Weighted Feedforward Scheme for Grid-Connected Inverter to Suppress the Injected Grid Current Harmonics Under Weak Grid," vol. 35, no. 9, pp. 9784–9793, 2020.

[6] S. W. Ali *et al.*, "Offshore Wind Farm-Grid Integration: A Review on Infrastructure, Challenges, and Grid Solutions," *IEEE Access*, vol. 9, pp. 102811–102827, 2021, doi: 10.1109/ACCESS.2021.3098705.

[7] L. Kangaji, E. Orumwense, and K. Abo-Al-ez, "Modelling and simulation of tidal energy generation system: a systematic literature review," *Int. J. Adv. Technol. Eng. Explor.*, vol. 9, no. 92, pp. 1028–1055, 2022, doi: 10.19101/IJATEE.2021.875704.

[8] L. Kangaji, E. Orumwense, and K. M. Abo-al-ez, "MODELLING AND PERFORMANCE ANALYSIS OF GRID CONNECTED TIDAL ENERGY GENERATION SYSTEM," pp. 1–6, 2021.

[9] A. I. Winter, "Differences in fundamental design drivers for wind and tidal turbines," *Ocean. 2011 IEEE - Spain*, 2011, doi: 10.1109/Oceans-Spain.2011.6003647.

[10] J. Adhikari, S. Member, I. V Prasanna, S. Member, S. K. Panda, and S. Member, "Voltage Oriented Control of the Three-level Vienna Rectifier Using Vector Control Method," *2016 IEEE Appl. Power Electron. Conf. Expo.*, pp. 9–16, 2016, doi: 10.1109/APEC.2016.7467845.

[11] J. Adhikari, I. V. Prasanna, and S. K. Panda, "Voltage oriented control of the three-level Vienna rectifier using vector control method," *Conf. Proc. - IEEE Appl. Power Electron. Conf. Expo. - APEC*, vol. 2016-May, pp. 9–16, 2016, doi: 10.1109/APEC.2016.7467845.

[12] X. Yu, Z. Cai, D. Ke, F. Wang, J. Rodriguez, and M. L. Heldwein, "Non-Cascaded Model-Free Predictive Direct Voltage Control of Three-Phase Vienna Rectifier," *2023 IEEE Int. Conf. Predict. Control Electr. Drives Power Electron. Preced. 2023*, pp. 1–6, 2023, doi: 10.1109/PRECEDE57319.2023.10174480.

[13] J. Adhikari, I. V. Prasanna, and S. K. Panda, "Reduction of input current harmonic distortions and balancing of output voltages of the Vienna rectifier under supply voltage disturbances," *IEEE Trans. Power Electron.*, vol. 32, no. 7, pp. 5802–5812, 2017, doi: 10.1109/TPEL.2016.2611059.

[14] A. Lunardi, E. Conde, J. Assis, L. Meegahapola, D. A. Fernandes, and A. J. Sguarezi Filho, "Repetitive Predictive Control for Current Control of Grid-Connected Inverter under Distorted Voltage Conditions," *IEEE Access*, vol. 10, pp. 16931–16941, 2022, doi: 10.1109/ACCESS.2022.3147812.

[15] Y. Gui, M. Li, J. Lu, S. Golestan, J. M. Guerrero, and J. C. Vasquez, "A Voltage Modulated DPC Approach for Three-Phase PWM Rectifier," *IEEE Trans. Ind. Electron.*, vol. 65, no. 10, pp. 7612–7619, 2018, doi: 10.1109/TIE.2018.2801841.

[16] J. Liu, S. Vazquez, L. Wu, A. Marquez, H. Gao, and L. G. Franquelo, "Extended State Observer-Based Sliding-Mode Control for Three-Phase Power Converters," *IEEE Trans. Ind. Electron.*, vol. 64, no. 1, pp. 22–31, 2017, doi: 10.1109/TIE.2016.2610400.

[17] S. Md. Mazhar-Ul-Haq, S. S. Tulasi Ram, and J. B. V. Subramanyam, "Voltage oriented control(VOC) of the PWM rectifier using active filtering function," *Int. J. Eng. Technol.*, vol. 7, no. 2.19 Special issue 19, pp. 90–93, 2018, doi: 10.14419/ijet.v7i2.19.15056.

[18] E. M. Suhara and M. Nandakumar, "Voltage oriented control of three phase PWM rectifier with Bus Clamped Space Vector PWM," *Proc. 2015 IEEE Int. Conf. Power, Instrumentation, Control Comput. PICC 2015*, vol. 43, pp. 5–9, 2016, doi: 10.1109/PICC.2015.7455788.

[19] A. Patil and S. Gadgune, "DC Side Voltage Regulation of Three Phase PWM Rectifier Control Using Sliding Mode Controller," *2022 Int. Conf. Futur. Technol. INCOFT 2022*, pp. 1–4, 2022, doi: 10.1109/INCOFT55651.2022.10094557.

[20] A. Kumar and G. Shankar, "Performance Analysis of Tidal Power Generation System on Load Frequency Control," *2018 13th Int. Conf. Ind. Inf. Syst. ICIIS 2018 - Proc.*, no. 978, pp. 387–391, 2018, doi: 10.1109/ICIINFS.2018.8721425.

[21] M. Al Razehi, R. Errouissi, M. Debouza, and H. Shareef, "Mitigation of 2ω-Ripple in DC-Link Voltage of PWM Rectifiers Under Unbalanced Grid Conditions," *IEEE Trans. Ind. Appl.*, vol. 59, no. 6, pp. 7608–7622, 2023, doi: 10.1109/TIA.2023.3299908.

[22] S. L. Sanjuan, "Voltage Oriented Control of Three - Phase Boost PWM Converters Voltage Oriented Control of Three - Phase Boost PWM Converters," 2010.

[23] M. Bhattacharya, "Improvement of Power Quality Using PWM Rectifier," *Int. J. Sci. Res. Publ.*, vol. 4, no. 7, pp. 1–11, 2014, [Online]. Available: https://www.semanticscholar.org/paper/Improvement-of-Power-Quality-Using-PWM-Rectifiers-Bhattacharya/10f29330a7ef4155e8d2c1721f1823d33c8fde37.

[24] A. S. Al-Ogaili *et al.*, "A three-level universal electric vehicle charger based on voltage-oriented control and pulse-width modulation," *Energies*, vol. 12, no. 12, 2019, doi: 10.3390/en12122375.

[25] K. P. Kumar, G. T. P. Naidu, and D. B. Chowdary, "Grid Connected Photovoltaic System with SVPWM Inverter Base on Voltage-Oriented Control at the Distribution System," pp. 515–521, 2016.

[26] T. Nguyen, H. Yoo, and H. Kim, "A Flywheel Energy Storage System Based on a Doubly Fed Induction Machine and Battery for Microgrid Control," pp. 5074–5089, 2015, doi: 10.3390/en8065074.

[27] Z. Ren, Y. Wang, H. Li, X. Liu, Y. Wen, and W. Li, "A Coordinated Planning Method for Micrositing of Tidal Current Turbines and Collector System Optimization in Tidal Current Farms," *IEEE Trans. Power Syst.*, vol. 34, no. 1, pp. 292–302, 2019, doi: 10.1109/TPWRS.2018.2865310.

[28] R. Teodorescu, M. Liserre, and P. Rodriguez, "Grid Converters for Photovoltaic and Wind Power Systems Chapter 10 Control of Grid Converters under Grid Faults," 2011.

[29] M. Malinowski, S. Stynski, W. Kolomyjski, and M. P. Kazmierkowski, "Control of Three-Level PWM Converter Applied to Variable-Speed-Type Turbines," *IEEE Trans. Ind. Electron.*, vol. 56, no. 1, pp. 69–77, 2009, doi: 10.1109/TIE.2008.927245.

[30] M. Elzalabani and A. E. A. E. Nafeh, "Modelling and Simulation of Tidal Current Turbine with Permanent Magnet Synchronous Generator," no. January, 2015, doi: 10.11591/telkomnika.v13i1.7017.

[31] M. Biweta and M. Mamo, "Closed loop control strategy of back to back PWM converter fed by PMSG using PLECS toolbox on Matlab/Simulink for wind energy application," *2017 IEEE AFRICON Sci. Technol. Innov. Africa, AFRICON 2017*, pp. 1313–1318, 2017, doi: 10.1109/AFRCON.2017.8095672.

[32] R. Brito, A. Carvalho, and M. Gericota, "A new three-phase voltage sourced converter laplace model," *Proc. - 2015 9th Int. Conf. Compat. Power Electron. CPE 2015*, pp. 160–166, 2015, doi: 10.1109/CPE.2015.7231066.